

The Physics of Brown dwarfs

G. Chabrier

Centre de Recherche Astrophysique de Lyon (UMR CNRS 5574),
Ecole Normale Supérieure de Lyon, 69364 Lyon Cedex 07, France

Abstract. We briefly outline the physics underlying the mechanical and thermal properties of brown dwarfs, which characterizes their interiors and their atmospheres. We mention the most recent improvements realized in the theory of brown dwarfs and the connection with experimental and observational tests of this theory.

1. Introduction

A general outline of the basic physics entering the structure and the evolution of brown dwarfs (BD) can be found in the previous reviews of Stevenson (1991) and Burrows & Liebert (1993). Important innovations have occurred in the field since then, one of the least negligible being the *discovery* of bona-fide brown dwarfs (Rebolo et al., 1995; Oppenheimer et al., 1995). An increasing number of these objects have now been discovered either as companions of stars, as members of young clusters or as free floating objects in the Galactic field (Ruiz et al., 1997; Delfosse et al., 1997). On the other hand the theory has improved substantially within the past few years and can now be confronted directly to observations and even to laboratory experiments, as will be shown below. It is thus important to reconsider the previous reviews in the light of these observational and theoretical progress and to update our knowledge of the structure and the evolution of BDs. This is the aim of the present review.

BDs are objects not massive enough to sustain hydrogen burning in their core and thus to reach thermal equilibrium, defined as $L = L_{nuc}$ where $L_{nuc} = \int_0^M \epsilon dm$ is the nuclear luminosity and ϵ is the nuclear reaction rate per unit mass. This hydrogen burning minimum mass M_{HBMM} depends on the internal composition of the object, in particular the abundance (by mass) of helium (Y) and heavier elements (Z). For abundances characteristic of the solar composition, typical of the Galactic disk population, $Y_{\odot}=0.27$ and $Z_{\odot}=0.02$, this minimum mass is $M_{HBMM} \sim 0.072 M_{\odot}$, whereas for compositions characteristic of the Galactic halo ($Y=0.25$; $Z \sim 10^{-2} \times Z_{\odot}$) $M_{HBMM} \sim 0.083 M_{\odot}$ (Chabrier & Baraffe, 1997; Baraffe et al., 1997) and for the zero-metallicity limit ($Z = 0$), $M_{HBMM} \sim 0.09 M_{\odot}$ (Saumon *et al.* , 1994).

The minimum mass for BDs is presently undetermined and masses as small as a Jupiter mass ($10^{-3}M_{\odot}$) are not excluded in principle. The divided line between BDs and giant planets (GPs) is still unclear and stems essentially from their formation processes :

hydrodynamic collapse of an interstellar molecular cloud for BDs, like for stars, accretion of heavy elements in a protostellar disk for the formation of planetesimals which eventually become dense enough to capture hydrogen and helium and form gaseous planets. The accretion scenario rather than the collapse scenario for the formation of planets is supported by the distinctly supersolar average abundance of heavy elements in Jupiter and Saturn, although there is only indirect evidence for the presence of the central rocky core through the modeling of the centrifugal moments. The border line between these two scenarios is presently unknown and involves most likely complex dynamical and non-linear effects. Extra-solar planets with masses as large as $\sim 40 M_J$ and BDs with masses as low as $\sim 30 M_J$ have now been discovered. Except for this formation process and for the presence of a central rock/ice core, the physics and the observational signature of BDs and GPs is very similar. Since a complete review is devoted to GPs (Stevenson, this issue), the present one will be devoted to BDs. In the present survey, I will focus on the most recent improvements realized in the physics of the interior and the atmosphere of BDs. I will also mention the physics underlying the so-called Lithium-test, which provides a powerful independent determination of the substellar nature and the age of a putative BD. The aim of the present review is not to present detailed calculations (which can be found in the various mentioned references) but rather to catch the underlying physics entering the structure and the evolution of BDs.

2. Interior of brown dwarfs. The hydrogen equation of state

Central conditions for massive BDs are typically $T_c \lesssim 10^5$ K and $\rho_c \sim 10^2$ - 10^3 g.cm⁻³. Under these conditions, the average ion electrostatic energy $(Ze^2)/a$, where $a = (\frac{3}{4\pi} \frac{V}{N_i})^{1/3}$ is the mean interionic distance, is several times the average kinetic energy kT , characterizing a strongly coupled ionic plasma with a coupling parameter $\Gamma_i = (Ze)^2/akT > 1$. The temperature is of the order of the electron Fermi temperature kT_F and the average inter-electronic distance a_e is of the order of both the Bohr radius $a_e \sim a_0$ and the Thomas-Fermi screening length $a_e \sim a_{TF}$. We thus have to deal with a partially degenerate, strongly correlated, polarizable electron fluid. The temperature in the envelope is $kT \lesssim 1$ Ryd, so we expect electronic and atomic recombination to take place. At last the electron average binding energy is or the order of the Fermi energy $Ze^2/a_0 \sim \epsilon_F$ so that *pressure-ionization* is taking place along the internal density profile.

Recently laser-driven shock-wave experiments have been conducted at Livermore (Da Silva et al., 1997; Collins *et al* , 1998) which probe directly the thermodynamic properties of dense hydrogen under conditions characteristic of BDs and GPs. The relevance of the Livermore experiments for the interior of these objects can be grasped from Figure 1. About a decade ago, Saumon & Chabrier (1991, 1992; SC) have developed a free energy model aimed at describing the thermodynamic properties of strongly interacting H₂ molecules, H atoms, H⁺ protons and electrons under such astrophysical conditions. The abundances of each species derive from the free energy

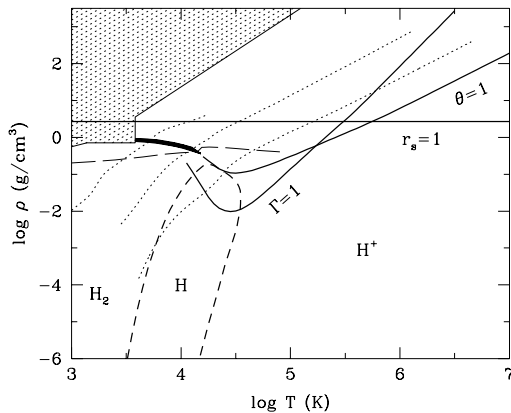


Figure 1. Phase diagram of hydrogen in $T - \rho$. The coexistence curve of the plasma phase transition (PPT) appears at the left of center as a black solid line which ends at the critical point. Curves of constant ionic (Γ) and electronic (r_s) plasma coupling parameter and electron degeneracy parameter $\theta = T/T_F$ are shown. Regions dominated by molecules, atoms and ionized H are labeled and delimited by a curve which corresponds to 50% dissociation and ionization. The calculated shock Hugoniot corresponding to the experiments is shown by the long-dash curve across the diagram. Finally, the thin dotted lines show the internal structure profiles of several astrophysical bodies (from left to right), Jupiter, a 7 Ga brown dwarf of $0.055 M_\odot$ and a $0.1 M_\odot$ star. The EOS model is invalid in the hashed region.

minimization :

$$\delta F(N_{H_2}, N_H, N_{H^+}, N_{e^-}, V, T) = \sum_i \frac{\partial F}{\partial N_i} \delta N_i = 0 \quad (1)$$

This model relies on the so-called chemical picture, which assumes that the species remain distinct even at high-density. This requires the knowledge of the interparticle potentials $\phi_{H_2H_2}$, ϕ_{H_2H} and ϕ_{HH} . Since N-body effects strongly modify the interaction between particles at high-density, "effective" pair-potentials can be derived from the experimental hugoniots. These effective pair-potentials mimic the softening of the interaction due to the surrounding particles and thus retain some density-dependence in the characteristic interactions between the main species. At the time the SC formalism was derived, the only available shock-wave experiments were the ones by Nellis et al. (1983). Since molecular dissociation was negligible under these conditions, only

an effective potential between H_2 molecules could be derived. The H_2 -H and H-H potentials were taken as ab-initio potentials. The more recent experiments by Weir et al. (1996) reach higher pressures and substantial molecular dissociation is inferred from these experiments ($X_H > 20\%$). This allows us to derive effective potentials for $\phi_{H_2H_2}$ and ϕ_{H_2H} as well and thus to update the SC model.

The recent laser-driven experiments have shown that the agreement between the *predictions* of the SC model and the data is excellent. In particular the strong compression factor arising from hydrogen pressure-dissociation and ionization observed in the experiment ($\rho/\rho_i \sim 5.8$) agrees well with the predicted theoretical value (Saumon et al., 1998). The compression is slightly underestimated in the theory and starts at a slightly too large pressure. This reflects the underestimated degree of dissociation in the model, which stems from the too repulsive (ab-initio) ϕ_{H_2H} potential at the time the SC model was elaborated. This shortcomings is resolved when including the afore-mentioned new effective H_2 - H_2 and H_2 -H potentials. Eventually full ionization is reached at very high pressure ($P \sim 10$ Mbar), characterized by the asymptotic compression factor $\rho_f/\rho_i = 4$ for a monoatomic fully dissociated proton fluid. These results show that, although this "chemical" model certainly does not pretend to give an exact, complete description of all the interactions in the high-pressure strongly correlated fluid, it very likely retains the main physics underlying the phenomenon of pressure-dissociation/ionization.

It is worthnoting that a similar strong compression factor is obtained also with the so-called fugacity expansion scheme, in principle exact in the strongly dissociated regime (Rogers and Young 1997), although this scheme fails at lower density when substantial recombination occurs.

One of the most striking features of the SC theory is the prediction of a first-order so-called plasma phase transition (PPT) between a molecular state and a plasma state for the pressure-ionization of hydrogen, similar to the one predicted originally by Wigner & Huntington (1935). However it is important to stress that the PPT in the SC model arises from first-principle thermodynamical instability of the one single free energy model ($(\partial P/\partial \rho)_T < 0$) and not from the comparison between two different free energy models. The new SC EOS, incorporating the new potentials, still predicts a PPT, although with a critical point slightly cooler than predicted previously, namely $T_c = 14600$ K, $P_c = 0.73$ Mbar (Saumon et al., 1998). In order to really nail down the existence of the PPT, we have calculated a second-shock Hugoniot reflected from the principal one, which should be realizable in a near future (Saumon et al., 1998). Such an experiment should confirm or rule out definitely the presence of the PPT.

The main question about the PPT is : if it exists, what is its nature ? This question has been addressed to some extend in Saumon & Chabrier (1992). If the PPT exists, it stems very likely from the large difference between a molecular state characterized by a strongly repulsive potential and a plasma state characterized by a soft Yukawa-like potential. Given the large difference between these two potentials, and thus the respective available phase spaces, we can expect a discontinuity in the interaction energy

and thus an abrupt change in the two-particle distribution function. This behaviour is observed in recent path-integral Monte-Carlo simulations (Magro et al., 1996; Ceperley, this issue). In terms of ground state energies, this translates into the large energy barrier between the ground state energy of an H_2 -like system (H_2 or H_2^+) and an H^+ -like system. In terms of correlation lengths that characterize the many-body effects, the system will collapse from a dense molecular phase characterized by a length $\lambda_{H_2} \sim$ a few a_0 into a plasma phase characterized by a length $\lambda_{H^+} \ll \lambda_{H_2}$. The underlying critical quantity will be the electron correlation length, with a critical percolation from a "bound-electron"-like value to a "free-electron"-like value. In this sense the PPT resembles the metal-insulator transition in metals associated with the liquid-vapor transition (Hensel, this issue), leading eventually to a polarization catastrophe (Goldstein & Ashcroft, 1985). The effect is likely to be more dramatic for hydrogen because of the absence of core electrons.

In this sense, the conductivity measurements of dense fluid hydrogen by Weir et al. (1996) do not rule out the PPT. The conductivity exhibits a plateau with $\sigma \sim 2000 (\Omega.cm)^{-1}$ up to the highest pressure reached, $P \sim 1.8$ Mbar. This is still orders of magnitude smaller than the conductivity characteristic of a fully dissociated plasma phase, $\sigma \sim 10^5 (\Omega.cm)^{-1}$ (Stevenson & Ashcroft, 1974) and is consistent with conduction being due to delocalized electrons from H_2^+ . This does not preclude a *structural* transition like the PPT at higher pressures.

If the PPT exists it can have important consequences for BDs and GPs. The interior of these objects is essentially isentropic. Since the signature of a first-order transition is a density and entropy discontinuity, integration along the internal adiabat from the observed outer conditions yields different central conditions with and without PPT (Chabrier et al., 1992). In principle the signature of the PPT in the interior of GPs like Jupiter and Saturn could be observed from the analysis of p-mode oscillations (Marley, 1994; Gudkova et al., 1995). However this requires very accurate observations of high-degree modes, a difficult observational task. The PPT bears also important consequences on the evolution of these objects. Since by definition BDs and GPs do not sustain hydrogen burning, application of the first and second principles of thermodynamics yields the following equation for their evolution :

$$L = -\frac{d}{dt} \int_0^M \left(\tilde{u} + \frac{P}{\rho^2} \frac{d\rho}{dt} \right) dm = -\int_0^M T \frac{d\tilde{s}}{dt} dm \quad (2)$$

where L is the luminosity, \tilde{u} and \tilde{s} the specific internal energy and entropy, respectively. If the PPT exists, an additional term, namely the latent heat of the phase transition, must be added to the previous equation :

$$L' = L + \int_{\Delta m} T \frac{d\Delta\tilde{S}}{dt} dm \quad (3)$$

This effect was first pointed out by Stevenson & Salpeter (1977) and examined in detail by Saumon et al. (1992).

3. The atmosphere of brown dwarfs

3.1. Spectral distribution

The photosphere is defined as the location where the photon mean free path is of the order of the mean interparticle distance, i.e. $l_\nu \sim 1/(\bar{\kappa}\rho) \sim a \propto \rho^{-1/3}$, where $\bar{\kappa} \sim 1\text{cm}^2/\text{g}$ is the mean absorption coefficient (opacity). This equality yields $l_\nu \sim a \sim 1\text{ cm}$. In terms of the dimensionless optical depth $\tau = z/l_\nu$, where z is the depth of the atmosphere, equilibrium between internal and gravitational pressure yields :

$$d\tau = -(\rho\bar{\kappa}) dz = \bar{\kappa} \frac{dP}{g}, \quad (4)$$

where $g = GM/R^2$ is the surface gravity. For BDs, $M \lesssim 0.1 M_\odot$, $R \sim 0.1 R_\odot$, $g \lesssim 10 \times g_\odot$. This yields $P_{ph} \sim g/\bar{\kappa} \sim 10\text{ bar}$ at the photosphere, and $\rho_{ph} \sim 10^{-5} - 10^{-4}\text{ g.cm}^{-3}$. Collision effects are significant under these conditions. Therefore thermodynamic equilibrium can be safely assumed near the photosphere. The bad news is that collision effects can induce dipoles between molecules, e.g. H_2 or He-H_2 , which otherwise would have only quadrupolar transitions. This so-called collision-induced absorption (CIA) between roto-vibrational states ($v \rightarrow v'$) of e.g. 2 H_2 molecules (1 and 2) can be written in terms of the 2-body absorption (see e.g. Borysow et al., 1985):

$$\begin{aligned} \kappa_{\text{H}_2\text{H}_2} &= \sum_{v_1, v'_1} \sum_{v_2, v'_2} \alpha_{\text{H}_2\text{H}_2}^{v_1, v'_1, v_2, v'_2}(\omega, T) \\ &= n_{\text{H}_2}^2 \frac{2\pi^2}{3\hbar c} w(1 - e^{-\hbar\omega/kT}) \sum_{v_1, v'_1} \sum_{v_2, v'_2} g^{v_1, v'_1, v_2, v'_2}(\omega, T) \end{aligned} \quad (5)$$

where $\omega = 2\pi\nu$ is the angular frequency, n_{H_2} is the number density of hydrogen molecules and $g^{v_1, v'_1, v_2, v'_2}(\omega, T)$ is the spectral function. We note the dependence on the square of the number abundance. As temperature decreases below $\sim 4000\text{ K}$, an increasing number of hydrogen molecules form and thus H_2 CIA-absorption becomes overwhelmingly important, a feature shared with giant planet and white dwarf atmospheres. Since the CIA absorption of H_2 under the conditions of interest for BDs and GPs takes place around $2.2\ \mu\text{m}$, energy conservation leads to a redistribution of the emergent radiative flux toward shorter wavelengths (Saumon et al., 1994; Baraffe et al., 1997).

The effective temperature is defined as the integral of the Eddington flux over the frequency spectrum :

$$T_{\text{eff}}^4 = \sigma^{-1} \int H_\nu d\nu, \quad (6)$$

where $\sigma = 5.67 \times 10^{-5}\text{ erg.cm}^2.\text{K}^4.\text{s}^{-1}$ is the Stefan-Boltzman constant. BDs are characterized by effective temperatures $T_{\text{eff}} \lesssim 2000\text{ K}$. At these temperatures, numerous molecules like e.g. H_2 , H_2O , TiO , VO , ... are stable and are the major absorbers of

photons. These strongly frequency-dependent opacity sources yield a strong departure from a black-body energy distribution (see e.g. Figure 5 of Allard et al. (1997)). An updated detailed review of the physics of the atmosphere of low-mass stars and BDs can be found in Allard et al. (1997).

Below $T \sim 1800$ K, carbon monoxide CO is predicted to dissociate and to form methane, CH_4 , as observed in Jupiter. This prediction has been confirmed by the discovery and the spectroscopic observation of Gliese229B. The presence of methane in its spectrum assessed unambiguously its sub-stellar nature. Consistent synthetic spectra and evolutionary calculations done both by the Lyon group (Allard et al., 1996) and the Tucson group (Marley et al., 1996) yielded the mass determination of the object between ~ 20 and $50 M_J$, the underdetermination in the mass reflecting the undetermination in the age of the system.

At last below ~ 2000 K complex compounds (grains, also called "clouds" by planetologists) condensate in the atmosphere (see e.g. Lunine et al., 1986; Tsuji et al., 1996). These grains will affect the atmosphere in different ways. They first modify the EOS itself and thus the atmospheric temperature/density-profile, and they also strongly affect the atmospheric opacity and thus the emergent radiation spectrum. At last they will produce an increase of the temperature in the uppermost layers of the atmosphere, the so-called backwarming (or greenhouse) effect, destroying otherwise stable polyatomic species. The condensation of the grains in a BD atmosphere is illustrated in Figure 2. Spectroscopic observations of different BDs at various effective temperatures show evidence for an even more complicated problem, namely grain diffusion (settling) in the atmosphere.

3.2. Energy transport

The radiative transport equation reads :

$$F_{rad} = \frac{4}{3\bar{\kappa}\rho} \frac{d}{dr} (\sigma T^4) \propto \frac{\nabla T}{\bar{\kappa}} \quad (7)$$

for the radiative flux, while convective transport can be written as :

$$F_{conv} \propto (\rho v_{conv}) \times (\tilde{c}_p \delta T) \quad (8)$$

where v_{conv} is the convection velocity, typically a fraction of the speed of sound, \tilde{c}_p is the matter specific heat at constant pressure and δT is the energy difference between the convective eddy and the surrounding ambient medium. As the temperature decreases below ~ 5000 K, which corresponds to a mass $m < 0.6 M_\odot$, H atoms recombine, n_{H_2} increases, and so does $\bar{\kappa}$ through H_2 CIA-absorption (see above). The opacity increases by several orders of magnitude over a factor 2 in temperature. On the other hand, the presence of molecules increases the number of internal degrees of freedom (vibration,

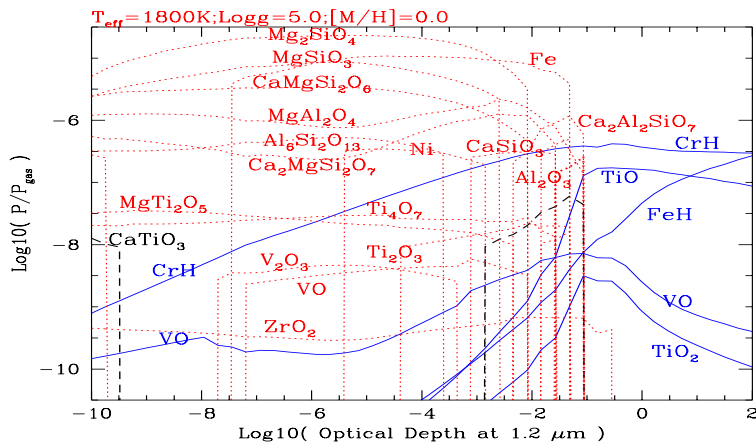


Figure 2. Relative abundances of gas phase (full lines) and crystallized species (dotted lines) across a $T_{\text{eff}} = 1800$ K brown dwarf model atmosphere (after F. Allard).

rotation, electronic levels) and thus c_p . These combined effects strongly favor the onset of convection in the optically-thin ($\tau < 1$) atmospheric layers. This can be shown easily from a stability (Schwarzschild) criterion analysis. Flux conservation thus reads :

$$\nabla(F_{\text{rad}} + F_{\text{conv}}) = 0 \quad (9)$$

i.e. no radiative equilibrium. The evolution of low-mass objects (low-mass stars, BDs, GPs) thus requires to solve the complete set of the transfer equations and to use consistent boundary conditions between the atmosphere and the interior structure profiles (Chabrier & Baraffe, 1997; Baraffe et al., 1995, 1997, 1998; Burrows et al., 1997).

4. Screening factors and the Lithium-test

Since a BD, by definition, never reaches thermal equilibrium ($L \sim T dS/dt$), age is an extra degree of freedom, yielding an undetermination in the mass and/or age of an object for a given observed luminosity and/or temperature. An independent age-indicator is thus needed. The presence of Lithium in the atmosphere of a cool object provides such an indication. The signature of Lithium absorption as a diagnostic for the sub-stellar nature of an object was first pointed out by Rebolo et al. (1992) while the measure of Lithium-depletion as an age tracer was first used by Basri et al. (1996).

The physics underlying the Lithium-test roots in dense plasma physics and in the calculations of the so-called nuclear screening factors for the nuclear reaction rate.

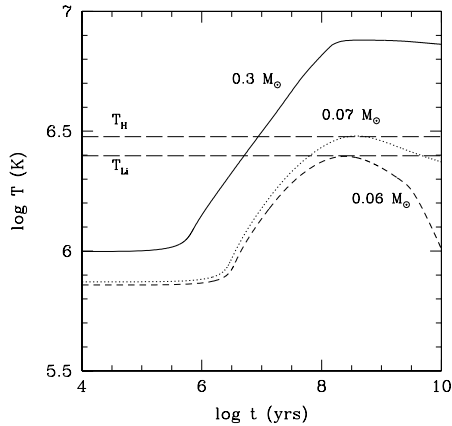


Figure 3. Central temperature as a function of age for 3 different masses respectively above, at the limit and below the hydrogen-burning minimum mass. T_H and T_{Li} indicate the Hydrogen and Lithium burning temperatures, respectively.

Primordial 7Li is destroyed through the nuclear reaction ${}^7Li + p \rightarrow 2{}^4He$. The reaction rate R_0 (in $\text{cm}^{-3}\text{s}^{-1}$) in the vacuum is given by the usual Gamow theory $R_0 \propto e^{-3\epsilon_0/kT}$ where ϵ_0 corresponds to the Gamow-peak energy for non-resonant reactions, which corresponds to the maximum probability for the reaction. However, as mentioned above, non-ideal effects dominate in the interior of BDs and lead to polarization effects in the plasma. These polarization effects due to the surrounding particles yield an enhancement of the reaction rate, as first recognized by Schatzman (1948) and Salpeter (1954). The distribution of particles in the plasma reads :

$$n(r) = \bar{n}e^{-Ze\phi(r)/kT} \quad (10)$$

with

$$\phi(r) = \frac{Ze}{r} + \psi(r) \quad (11)$$

where $\psi(r)$ is the induced mean field potential due to the polarization of the surrounding particles. This induced potential lowers the Coulomb barrier between the fusing particles and thus yields an *enhanced* rate in the plasma $R = E \times R_0$ where

$$E = \lim_{r \rightarrow 0} \left\{ g_{12}(r) \exp\left(\frac{Z_1 Z_2 e^2}{rkT}\right) \right\} \quad (12)$$

is the enhancement (screening) factor and $g_{12}(r)$ the pair-distribution function.

Under BD conditions, not only *ionic* screening must be included but also *electron* screening, i.e. $E = E_i \times E_e$. Both effects are of the same order ($E_i \sim E_e \sim \text{a few}$)

and must be included in the calculations for a correct estimate of the Lithium-depletion factor $[Li]_0/[Li]$, where $[Li]_0 = 10^{-9}$ denotes the primordial Lithium-abundance. This yields a Lithium-burning minimum mass $m_{Li} \sim 0.06 M_{\odot}$ (Chabrier & Baraffe, 1997), *below* the hydrogen-burning minimum mass, as illustrated in Figure 3. After the common primordial deuterium burning phase, which lasts $\sim 10^6 - 10^7$ yr, the central temperature evolves differently, depending on the mass of the object. Note the strong age dependence of the Lithium-test : young *stars* with an age $t \lesssim 10^8$ yr (depending on the mass) will exhibit Lithium, whereas massive *brown dwarfs* within the mass range $[0.06-0.07 M_{\odot}]$ older than $\sim 10^8$ yr will have burned Lithium. The measure of Lithium depletion in the atmosphere of low-mass objects, inferred from the width of the LiI line at 6708 \AA , as an age indicator, is illustrated in Figure 4. This figure displays the evolution of a $0.075 M_{\odot}$ object, the H-burning limit for solar-abundances, in the I-band magnitude. The left and right diagonal solid lines correspond to 50% Li-depletion ($[Li]_0/[Li] = 1/2$) and 99% Li-depletion, respectively. Thus, for say 120 Myr, the inferred age of the Pleiades cluster, objects brighter than $M_I \sim 12.2$ will lie on the right-hand side of the 99%-depletion line and thus are predicted to show no Lithium in their atmosphere and to be H-burning stars ($m \geq 0.075 M_{\odot}$), whereas objects fainter than this magnitude will all show *some* Lithium and all be brown dwarfs ($m < 0.075 M_{\odot}$ for this age), with objects fainter than $M_I \sim 12.6$ predicted to have retained more than half their primordial Lithium-abundance. The horizontal lines show the observed magnitudes of 4 different objects in the Pleiades, with available high-resolution spectra. All four confirm the theory, with no Lithium observed for PL10, about 50% depletion for PL13 and negligible or no depletion for Roq13 and Teide1. Different isochrones for different masses can be superimposed on the same diagram and analyzed similarly. This illustrates convincingly the powerful diagnostic of Lithium as a mass and age indicator for low-mass stars and brown dwarfs.

5. Conclusion

As a conclusion to this review, I will list a series of "homework problems" related to BDs which illustrate the major problems to be addressed in this field in a near future and which correspond to different domains of physics or astronomy. This list is certainly not exhaustive.

- *Dense matter physics:* As we have seen, BD interiors can now be tested directly in laboratories and the EOS of these objects can be probed by high-pressure experiments. More experiments are needed in the complex regime of H-pressure dissociation/ionization with several unanswered questions. Does the PPT really exist ? Does it survive when 10% helium particles are present ? How does pressure-ionization of H affect the dynamo process in BD and GP interiors ?

- *Star formation process:* Jeans stability analysis yields a minimum mass $m_{min} \sim 0.01 M_{\odot}$, definitely in the BD domain (Silk, 1977). Is this mass the BD minimum mass ? Conversely what is the maximum mass for planet formation ? Does the Jeans criterion really apply for the formation of star-like objects ? What is the BD *mass function* in

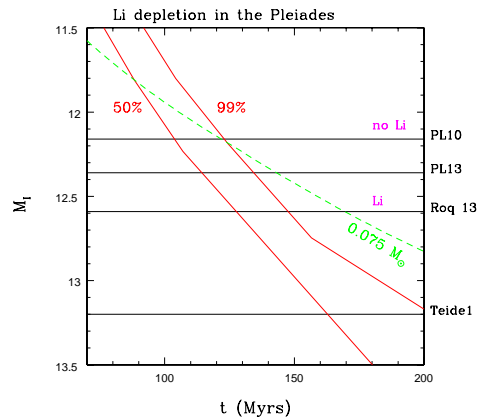


Figure 4. Evolution of the absolute magnitude M_I as a function of age. The dashed line corresponds to the hydrogen-burning minimum mass, whereas the diagonal solid lines correspond to the 50% et 99% Lithium-depletion limit. The horizontal solid lines indicate the observed magnitudes of different low-mass objects.

the Galaxy ?

- *Evolution:* The evolution of BDs is not hampered by any adjustable parameter, like for example in the treatment of convection for more massive stars which develop an inner radiative core. The theory of BDs, and the comparison with observation, thus reflects the validity of the very physics entering the theory, both in the atmosphere and in the interior. This theory can be tested directly now by photometric and spectroscopic observations and must address new problems like e.g. the diffusion process of grains in the atmosphere or the magnetic field generation in active BDs. Conversely, the theory is now reliable enough to provide useful guidance for future observations.

- *Galactic implication:* The mass-to-light ratio for BD, $(M/L)_{BD} \gtrsim 10^4 (M/L)_{\odot}$, make BDs very promizing candidates to explain at least the baryonic missing mass. Even though present estimates of their contribution to the Galactic disk and halo mass seem to exclude this possibility (Chabrier & Méra, 1997; Méra et al., 1998), the determination of their exact number- and mass-density in the Galaxy remains to be determined accurately. Ongoing microlensing experiments sensitive to hours and day event durations and ongoing wide field infrared projects (e.g. DENIS, 2MASS) will certainly help nailing down this issue.

BDs thus present a wide variety of interest from basic physics to Galactic implications and should remain a very active field.

5.1. Acknowledgments :

The results mentioned in this review to illustrate the physics of BDs arise from an ongoing collaboration with F. Allard, I. Baraffe and P.H. Hauschildt for the structure and the evolution of BDs, and with D. Saumon for the EOS. My profound gratitude to these persons for their contribution to this review.

References

- Allard, F., Alexander, D., Hauschildt, P.H. & Starrfield, S., 1997, *ARA&A* **35**, 137
 Allard, F., Hauschildt, P.H., Baraffe, I. & Chabrier, G., 1996, *Astroph. J.*, **424**, 333
 Basri, G., Marcy, G., & Graham, J. R., 1996, *Astroph. J.*, **458**, 600
 Baraffe, I., Chabrier, G., Allard, F. & Hauschildt, P.H., 1995, *Astroph. J.*, **446**, L35
 Baraffe, I., Chabrier, G., Allard, F. & Hauschildt, P.H., 1997, , *Astron. & Astroph.*, **327**, 1054
 Baraffe, I., Chabrier, G., Allard, F. & Hauschildt, P.H., 1998, , *Astron. & Astroph.*, 337, 403
 Borysow, A., Trafton, L., Frommhold, L. & Birnbaum, G., 1985, *Astroph. J.*, **296**, 644
 Burrows, A., Marley, M., Hubbard, W.B., Lunine, J.I., Guillot, T., Saumon, D., Freedman, R., Sudarsky, D., Sharp, C. 1997, *Astroph. J.*, **491**, 856
 Burrows, A. & Liebert, J., 1993, *Rev. Mod. Phys.*, **65**, 301
 Chabrier, G & Baraffe, I., 1997, *Astron. & Astroph.*, **327**, 1039
 Chabrier, G & Méra, D., 1997, *Astron. & Astroph.*, **328**, 83
 Chabrier, G., Saumon, D., Hubbard, W.B. & Lunine, J.I., 1992 *Astroph. J.* **391**, 817
 Collins, G.W., *et al* , 1998, *Science*, **281**, 1178
 Goldstein R.E. & Ashcroft, N. W., 1985, *Phys. Rev. Lett.*, **55**, 2164
 Da Silva, L.B., *et al.*, 1997, *Phys. Rev. Lett.*, **78**, 483
 Delfosse, X. *et al.*, 1997, *Astron. & Astroph.*, **327**
 Gudkova, T., Mosser, B., Provost, J., Chabrier, G., Gautier, D. & Guillot, T., 1995, *Astron. & Astroph.*, **303**, 594
 Lunine, J.I., Hubbard, W.B., and Marley, M.S., 1986, *Astroph. J.*, **310**, 238
 Magro, W.R., Ceperley, D.M., Pierleoni, C., & Bernu, 1996, *Phys. Rev. Lett.* **76**, 1240
 Marley, M.S., Saumon, D., Guillot, T., Freedman, R., Hubbard, W.B., Lunine, J.I. & Burrows, A., 1996, *Science*, **272**, 1919
 Marley, M.S., 1994, *Astroph. J.*, **427**, L63
 Méra, D., Chabrier, G. & Schaeffer, R., 1998, *Astron. & Astroph.*, **330**, 937; , **330**, 953
 Nellis, W.J., Mitchell, A.C., van Thiel, M., Devine, G.J., & Trainor, R.J., 1983, *J. Chem. Phys.* **79**, 1480
 Oppenheimer, B.R., Kulkarni, S.R., Nakajima, T. & Matthews, K., 1995, *Science*, **270**, 1478
 Rebolo, R., Martín, E.L., Magazzù, A, 1992, *Astroph. J.*, **389**, 83
 Rebolo, R., Zapatero Osorio, M.R. & Martin, E.L., 1995, *Nature*, **377**, 83
 Rogers, F. & Young D., 1997, *Phys. Rev. E* **56**, 5876
 Ruiz, M.-T., Leggett, S. & Allard, F., 1997, *Astroph. J.*, **491**, L107
 Salpeter, E.E., 1954, *Austral. J. Physics*, **7**, 373
 Saumon, D. & Chabrier, G., 1991, *Phys. Rev. A* **44**, 5122; 1992, *Phys. Rev. A* **46**, 2084
 Saumon, D., Bergeron, P., Lunine, L.I., Hubbard, W.B., and Burrows, A., 1994, *Astroph. J.*, **424**, 333
 Saumon, D., Hubbard, W.B., Chabrier, G. & Van Horn, H.M., 1992, *Astroph. J.* **391**, 827
 Saumon, D., Chabrier, G., Wagner, D.J., and Xie, X., 1998, *Phys. Rev.*, submitted
 Schatzman, E., 1948, *J. Phys. Rad*, **9**, 46
 Silk, J., 1977, *Astroph. J.* **211**, 638
 Stevenson, D., 1991, *ARA&A* **29**, 163
 Stevenson, D. & Ashcroft, N. W., 1974, *Phys. Rev. A* **9**, 782

- Stevenson, D.J. & Salpeter, E.E., 1977, *Astroph. J. Supp.* **35**, 221
Tsuji, T., Ohnaka, K., and Aoki, W., 1996, *Astron. & Astroph.* **305**, L1
Weir, S.T., Mitchell, A.C., & Nellis, W.J., 1996, *Phys. Rev. Lett.* **76**, 1860
Wigner, E. & Huntington, H.B. 1935, *J. Chem. Phys.* **3**, 764